Disulfide Connectivity of Human Immunoglobulin G2 Structural Isoforms

Theresa Martinez,[‡] Amy Guo,[‡] Martin J. Allen,[§] Mei Han,[‡] Danielle Pace,[‡] Jay Jones,[‡,||] Ron Gillespie,[⊥] Randal R. Ketchem,[#] Yuling Zhang,[‡] and Alain Balland*[,‡]

Process and Product Development, Amgen, Inc., Seattle, Washington 98119

Received April 2, 2008; Revised Manuscript Received May 13, 2008

ABSTRACT: In this communication we present the detailed disulfide structure of IgG2 molecules. The consensus structural model of human IgGs represents the hinge region positioned as a flexible linker connecting structurally isolated Fc and Fab domains. IgG2 molecules are organized differently from that model and exhibit multiple structural isoforms composed of (heavy chain−light chain−hinge) covalent complexes. We describe the precise connection of all the disulfide bridges and show that the IgG2 C_H1 and C-terminal C_L cysteine residues are either linked to each other or to the two upper hinge cysteine residues specific to the IgG2 subclass. A defined arrangement of these disulfide bridges is unique to each isoform. Mutation of a single cysteine residue in the hinge region eliminates these natural complexes. These results show that IgG2 structure is significantly different from the conventionally accepted immunoglobulin structural model and may help to explain some of the unique biological activity attributed only to this subclass.

The three-dimensional structures of the Fab and Fc domains of IgG molecules have been solved through numerous studies by X-ray diffraction studies of crystal fragments (*1, 2*). The overall structure of the IgG family is organized in 12 immunoglobulin domains each closed by an intrachain disulfide bond (reviewed in refs *3* and *4*). Fab and Fc regions are connected by the hinge, an area important for the flexibility of the molecule and its adaptability to various presentations of antigen targets. The hinge is divided into three regions: upper, core, and lower. The core cysteines are involved in inter-heavy chain disulfide bonding responsible for the covalent complex of the form $(HC\text{-}LC)_2$.[1] Sequence comparison indicates that immunoglobulin subclasses exhibit differences in the genetic hinge region in the length and number of cysteine residues. IgG1 (15 residues) and IgG2 and IgG4 (12 residues each) are relatively comparable in size whereas, due to domain duplication, IgG3 is unique with a long hinge of 62 amino acids including 11 cysteines. IgG1 and IgG4 hinge core sequences are very similar with 2 cysteines on each heavy chain involved in inter-heavy chain connection. Specific residues of the hinge region have been shown to have profound impact on the properties of immunoglobulins. For example, the presence of serine in the canonical core structure, CPXCP, explains the unique property of IgG4 molecules to form HC-LC half-structures (*5*). A recent report has shown that this property allows a dynamic exchange of the hinge disulfides *in vivo* resulting in bispecific IgG4 antibodies (*6*). IgG2 is unique in presenting 4 cysteine residues in the hinge region, notably two consecutive residues, Cys-232 and Cys-233 (Kabat numbering (*7*)) that have no equivalent in any other immunoglobulin subclass. We show in this report that these residues confer distinctive structural features to the IgG2 subclass.

The IgG1 covalent structure is schematically presented in Figure 1A. Resolving intact antibody structures by X-ray diffraction analysis has proved difficult, and only three structures of complete antibodies with hinge are known to date (*8–10*). In contrast to human IgG1, detailed structural analysis of human IgG2 is very limited, and there are no published human IgG2 structures that include the hinge region. Most information about the hinge of this subclass is derived by homology modeling using human IgG1 and murine IgG1 and IgG2. Based on known X-ray structures of murine antibodies that show the three cysteine residues of the murine hinge region to be involved in inter-heavy chain disulfide bridges (*9*), a general organization of human IgG2 has been derived as schematically shown in Figure 1B. This consensus model is supported only by limited biochemical studies of enzymatic digests of myeloma protein (*11*). These studies describe the disulfide connection of the cysteine residues in the core region organized in parallel.

We recently reported that studies of the covalent structure of IgG2 molecules performed at Amgen indicate that the consensus structural model of human IgG2 is only a minor form, among several disulfide-related structural isoforms (*12, 13*). In this communication, we investigated the precise cysteine connectivity of each isoform. The experiments were performed on a recombinant IgG2 molecule produced at large manufacturing scale and led to a complete description of the

* Corresponding author: tel, (206) 265-8603; fax, (206) 217-4692; e-mail, ballanda@amgen.com.

[‡] Department of Analytical and Formulation Sciences.

[§] Department of Cell Sciences and Technology.

[||] Present address: Seattle Genetics, 21823 30th Drive SE, Bothell, WA.

[⊥] Department of Purification Process Development.

[#] Department of Protein Sciences.

[1] Abbreviations: mAb, monoclonal antibody; HC, heavy chain; LC, light chain; RP, reversed phase; LC-MS, liquid chromatography−mass spectrometry; nrCE-SDS, nonreduced capillary electrophoresis sodium dodecyl sulfate; dSEC, denaturing size exclusion chromatography; CEX, cation-exchange chromatography; IAA, iodoacetic acid; NEM, *N*-ethylmaleimide; Gal, galactose.

10.1021/bi800576c CCC: $40.75
Published on Web 06/13/2008

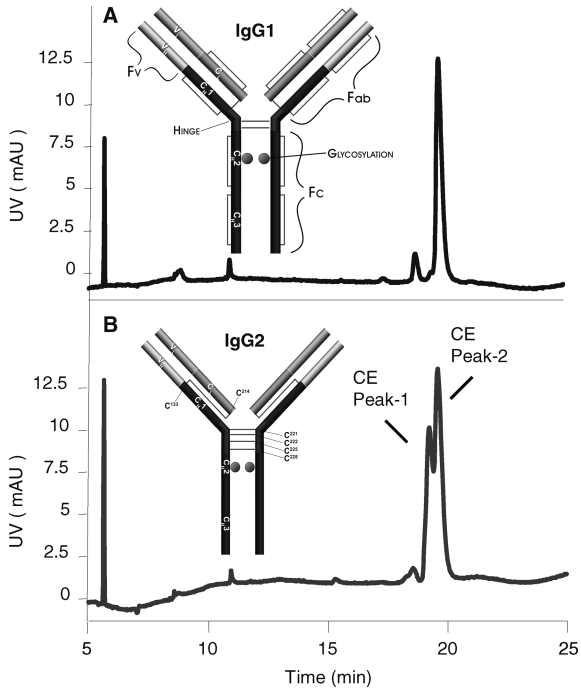

FIGURE 1: Schematic structures and nonreduced CE-SDS separation of IgG1 and IgG2 subclasses. (A) IgG1 model depicting the structural features of immunoglobulins. Nonreduced CE-SDS resolves IgG1 molecules in a single peak. (B) The structural model of IgG2 antibodies defines a covalent association of heavy chain and light chain by one disulfide bond and a final quaternary structure of the form $(HC\text{-}LC)_2$ maintained by four inter-heavy chain disulfide bonds in the hinge region of the heavy chains. The cysteine residues are numbered according to the IgG2 sequence, (LC) C^{214} and (HC) C^{133}, C^{221}, C^{222}, C^{225}, C^{228}. A doublet of different structural species is observed for IgG2 antibodies by nrCE-SDS. The other minor species detected in this method represent nonglycosylated species and different stochiometry of heavy and light chains, not relevant to the concept of structural isoforms.

disulfide connectivity patterns. Furthermore, we present evidence that site-directed mutagenesis of a single cysteine residue in the upper hinge selectively eliminates these structural isoforms.

MATERIALS AND METHODS

Fully human monoclonal antibodies were manufactured at Amgen (Seattle, WA). The endoproteinase enzymes were obtained from Roche. The commercial myeloma IgG2 was purchased from Sigma. CE reagents, run buffer, reference standard, and sample buffer were obtained from Bio-Rad.

Capillary Electrophoresis Methods. The analyses were performed on an HP^{3}D CE system (Agilent Technologies, Palo Alto, CA) equipped with a diode array detector. Separations were performed using a bare-fused silica capillary with a total length of 33.0 cm, effective length of 24.5 cm, with an inner diameter (i.d.) of 50 μm and outer diameter (o.d.) of 365 μm. Antibody separation was monitored at a wavelength of 220 nm.

Nonreduced Capillary Electrophoresis Sodium Dodecyl Sulfate (nrCE-SDS). The antibody samples at a minimum concentration of 2.5 mg/mL were diluted to a final concentration of 1 mg/mL according to the following procedure: 150 μg of antibody solution was combined to 15 mM iodoacetamine (IAM), 3 μL of internal standard (benzoic acid; Bio-Rad) was added, and the solution was brought to 150 μL with CE-SDS sample buffer (Bio-Rad). The solution was mixed, centrifuged, and heated at 75 °C in water bath for 10 min. The mixture was cooled at room temperature, centrifuged at 12000 rpm for 6 min, and transferred to sample vials for injection.

Reduced Capillary Electrophoresis Sodium Dodecyl Sulfate (rCE-SDS). The antibody samples were prepared as described above with 10 μL of neat β-mercaptoethanol (β-ME) in lieu of iodoacetamine.

CE Separation Conditions. The capillary was preconditioned with 0.1 N NaOH at 6 bar for 2 min followed by 0.1 N HCl treatments at 6 bar for 1.5 min to neutralize silanol groups. The capillary was filled with Bio-Rad CE-SDS run buffer at 6 bar for 3 min. Samples were injected at −10 kV for 20 s and separated at −15 kV for 30 min.

Redox (Cysteine/Cystine) Treatment. Samples were treated with 6 mM cysteine and 0.6 mM cystine in 0.2 M Tris-HCl at pH 8.6 for 96 h at 2−8 °C. Samples were then dialyzed into their formulation buffers. Human IgG2 was dialyzed into its original formulation buffer, 40 mM phosphate and 150 mM NaCl, pH 7.4.

Preparative Scale CEX Fractionation. Material was buffer exchanged into 50 mM sodium acetate, pH 5, using a Centriprep YM-10 centrifugal membrane. Material was applied to the Fractogel EMD SO3 preparative CEX resin obtained from Merck (1.6 cm deep × 25 cm high) at a 20 g/L resin load and eluted in 50 mM sodium acetate, pH 5, over a 15 column volume linear gradient from 0 to 300 mM sodium chloride. Fractions were collected throughout the gradient elution in 10 mL increments. The separation was performed on a Bio-Rad chromatography system.

Semipreparative scale CEX Fractionation. Fractions isolated from preparative CEX were buffer exchanged to 20 mM MES, pH 6, by dialysis using Pierce 10K MWCO Slide-a-Lyzer dialysis cassettes followed by concentration to approximately 30 mg/mL using a 50K MWCO Amicon Ultra-15 centrifugal filter device. Further separation was performed on a WCX-10 semiprep CEX column (9−250 mm) obtained from Dionex, using a sodium chloride conditional step gradient from 0 to 70 mM NaCl in 20 mM MES, pH 6, followed by a 20 mM MES/1 M NaCl, pH 6, wash.

Tryptic Peptide Mapping of the Nonreduced Molecule. Potential free cysteine residues present on the monoclonal antibody were alkylated with *N*-ethylmaleimide (NEM). The NEM-labeled material was digested with 10% (w/w) trypsin in 0.1 M Tris/2 M urea, pH 8.3, at a concentration of 1 mg/mL for 4 h at 37 °C. The digest reaction was quenched with the addition of 10 μL of 10% TFA.

The trypsin-digested sample was analyzed via RP-HPLC with column heating at 60 °C. Mobile phases consisted of (A) 0.12% TFA in water (w/v) and (B) 0.11% TFA in 40:40:20 acetonitrile:2-propanol:water (w/v). Separation was performed on a Jupiter C5 (2.1 × 250 mm) column, conditioned in mobile phase A for 20 min. Digest (100 μg) was injected, and the peptide fragments were eluted at a flow rate of 0.2 mL/min with a gradient of 0−65% B in 165 min.

Peptide elution was monitored by UV absorbance at 214 nm and online mass acquisition.

Reduction and Alkylation Protocol. The trypsin-digested material was reduced with dithiothreitol (DTT) for 30 min at 55 °C. The antibody was then alkylated with iodoacetic

acid (IAA) for 15 min at room temperature. The alkylation reaction was quenched with the addition of DTT.

Mass Spectrometry Conditions for Peptide Mapping. All analyses were performed using a LCQ Deca ion-trap instrument (Thermo-Finnigan, San Jose, CA) equipped with an electrospray source connected to an Agilent 1100 pump (Agilent Technologies, Palo Alto, CA). Analysis was carried out in positive ion mode using a spray voltage of 5.0 kV, and the MS capillary temperature was maintained at 225 °C. The instrument was calibrated in the *m*/*z* range of 500−2000 using a mixture of caffeine, MRFA peptide, and Ultramark 1621. Deconvolution of electrospray ionization mass spectra for the heavy and light chain was done using ProMass for Xcalibur software.

Spectral data for the protein digests were acquired online in the range 200−2000 *m*/*z*. MS/MS analysis was performed in data-dependent mode. Collision data were obtained using 40% relative collision energy.

Whole Mass Analysis Protocol. This technique was applied as described recently (*14*). Samples were introduced into the mass spectrometer by isocratic separation on a polyhydroxyethylaspartamide column flowing at 0.1 mL/min in 0.1% (v/v) formic acid. Samples eluted as a single peak separated from salt and buffer components. A solution of 1% (v/v) formic acid in acetonitrile was mixed into the column eluate at 25 μL/min by use of a syringe pump and a tee. The column eluate was directed into an ESI-TOF mass spectrometer (Agilent Technologies, Palo Alto, CA) with divert valve settings selected to direct salt and buffer components to waste. The instrument was tuned and calibrated using Agilent supplied tuning and calibration solution from 50 to 4000 *m*/*z*. Optimized source and ion transmission system conditions were empirically determined and included a capillary voltage of 5000 V, nitrogen gas rate of 9.0 L/min, and a fragmentor voltage of 415 V. Other settings were typical for this instrument.

Construction and Production of Cys→Ser Mutants. Site-directed mutagenesis was performed using a QuickChange site-directed mutagenesis kit (Stratagene, La Jolla, CA), and the presence of the desired mutations was confirmed by DNA sequencing. Expression plasmids with the desired mutation were stably transfected into suspension-adapted CHO cells deficient in dihydrofolate reductase activity. Cells expressing the antibody of interested were selected by growth in medium lacking glycine, hypoxanthine, and thymine. Following recovery from transfection and selection, CHO cell pools were grown in production spinner flasks. Expressed antibody was purified from harvested cell culture supernatant by protein A affinity chromatography and characterized as described.

IgG2 C_H1 and Hinge Illustration. To illustrate the close proximity of the IgG2 C_H1 Cys residue (Cys-133) with the hinge residues Cys-221 and Cys-222 and the interchain disulfide bonding LC Cys residue (Cys-214), Figure 2 was constructed as follows:

The C_H1 amino acid sequence of the recombinant IgG2 was modeled against the known C_H1 structure of an IgG4 antibody (pdb accession code 1ad9 (*15*)); the amino acid sequence identity between the C_H1 sequence of IgG2 and the template is 96%, and the positions and identity of all Cys residues are absolutely conserved. The resulting IgG2 C_H1 model was superposed onto the C_H1 structure of a human IgG1 that includes the hinge region (pdb accession code 1hzh (*16*)). The IgG2 C_H1 model was then computationally fused to the IgG1 structure at the end of the C-terminal β-strand of the C_H1 domain to produce a pseudo-IgG2 C_H1 and hinge. The amino acids remaining from the IgG1 structure were then computationally mutated to their corresponding residues in the IgG2 sequence to produce the final IgG2 C_H1 and hinge illustration. The positions of the LC Cys residue from an IgG1 or IgG4 were taken from the 1hzh and 1ad9 structures, respectively; it is noteworthy that the constant light chain domain of 1ad9 is identical to that of the IgG2 and the constant light chain domain of 1hzh differs from this molecule at only a single residue distant from Cys-214. The light chain Cys residues shown in Figure 2 differ in their orientation. However, flexibility at this residue is expected since it is the last amino acid in the light chain. Three-dimensional modeling was performed using MOE (Chemical Computing Group, Montreal, Quebec, Canada), and Figure 2 was produced using the PyMOL Molecular Graphics System (DeLano Scientific, San Carlos, CA).

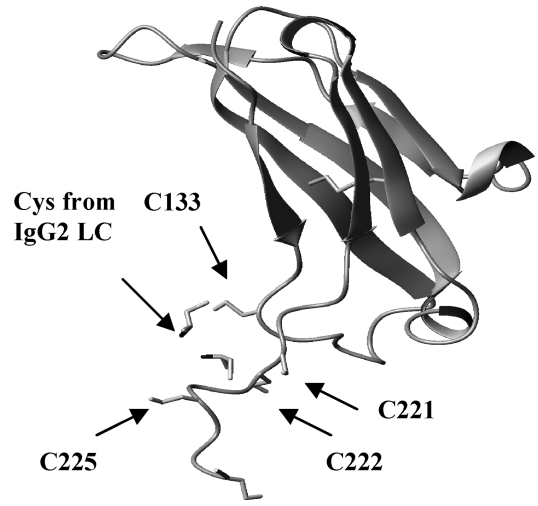

FIGURE 2: Three-dimensional model illustrating the C_H1 and hinge region of a single IgG2 heavy chain. Also shown is the LC Cys residue that disulfide bonds with the heavy chain from the published structure of an IgG1 Fab. To illustrate one possible orientation of the LC Cys residue in human IgG2, the position of the LC residue of a human IgG4 Fab is shown. The C_H1 Cys that disulfide bonds to the LC in human IgG4 aligns with the position of the Cys-133 in human IgG2.

RESULTS

We evaluated the apparent size of antibodies by nonreduced capillary electrophoresis sodium dodecyl sulfate (nrCE-SDS), a gel sieving method performed on fully denatured molecules. We found that this technique has unique ability to resolve immunoglobulins (*17*). Electropherograms of IgG1 and IgG2 molecules (Figure 1) show that nrCE-SDS generates different results depending on the antibody subclass. IgG1 is resolved in a single, homogeneous main peak (Figure 1A), whereas IgG2 exhibits a specific heterogeneity resulting in the separation of two main species (Figure 1B). As nrCE-SDS technique separates biomolecules based on their hydrodynamic size under denaturing and nonreduced conditions, we conclude that IgG2, in contrast to IgG1, is composed of molecular species with different covalent structures. The recombinant IgG2 was found to contain a 40:60 ratio of CE isoform peak 1 to CE isoform

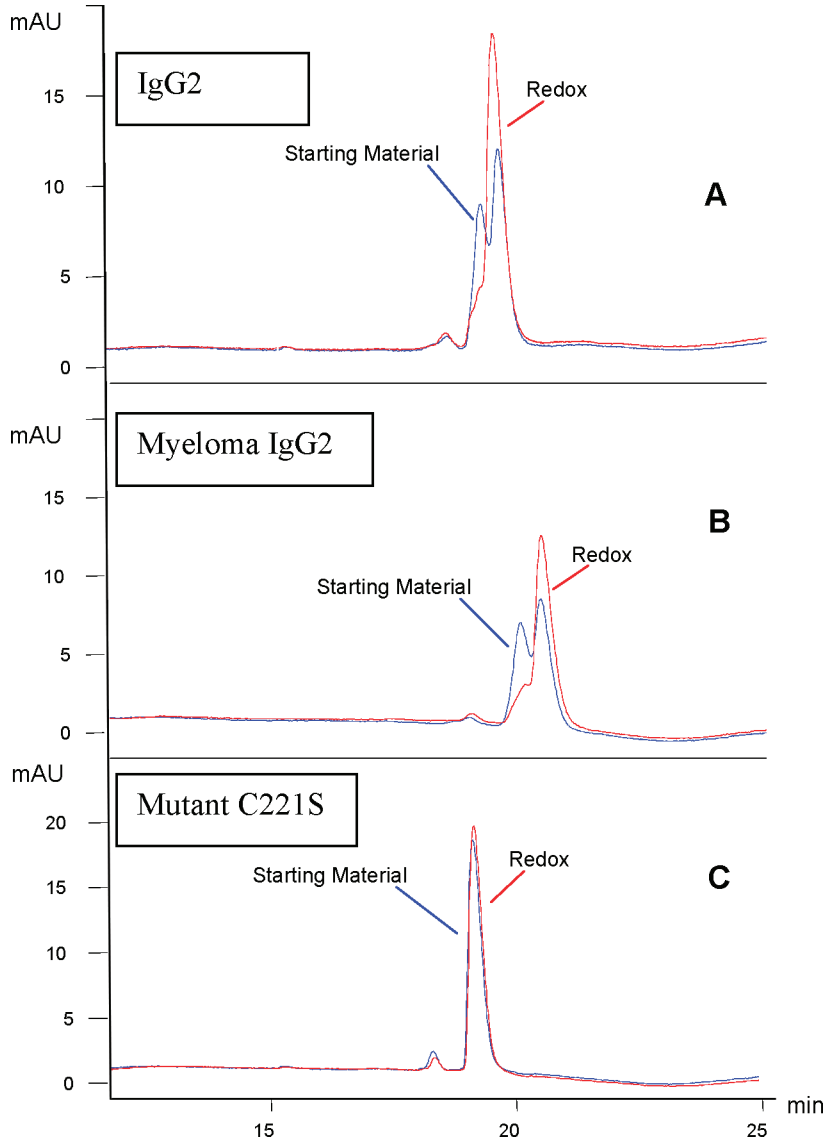

FIGURE 3: Separation of IgG2 molecules by nrCE-SDS. (A) recombinant IgG2 and (B) commercially available human IgG2 isolated from serum of myeloma patient exhibit the doublet typical of structural isoforms (blue traces). Application of cysteine/cystine redox potential leads to rearrangement of disulfide bridges, resulting in decrease of isoform 1 and increase of isoform 2 (red traces). (C) Single cysteine mutants (C221S and C222S) are resolved in a single peak expected of a homogeneous structure. The treatment by redox potential does not affect the mutants devoid of structural isoforms.

peak 2 by UV integration. Commercially available human IgG2 purified from serum of myeloma patients (Sigma, St. Louis, MO) displayed the typical doublet profile observed for recombinant IgG2 molecules. The isoforms were shown to be dependent on the presence of the complete covalent structure of the form $(HC\text{-}LC)_2$. Application of a cysteine: cystine redox potential (Figure 3) modified the structural isoforms, resulting in a significant decrease of isoform peak 1 (40% to 12%) concomitant with an increase of isoform peak 2 (60% to 88%). This result suggests that the isoforms present in peaks 1 and 2 are distinct and are based on disulfide bond arrangements.

CEX Isolation of Structural Isoforms. In order to obtain large amounts of sufficiently pure material for further characterization and identification of the isoforms and complex disulfide-linked, IgG2 molecule was fractionated by cation-exchange chromatography (CEX) at preparative scale. CEX was an appropriate method to separate the isoforms as the separation mechanism was found to be based on both surface charge and structural features of the IgG2 molecule. The material was applied to a preparative CEX column and eluted at pH 5 with a gradient of sodium chloride. Preparative fractions were collected in 10 mL increments and analyzed by nrCE-SDS. The nrCE-SDS results demonstrated that enrichment in isoform 1 was observed in mid-to-later (basic) fractions and enrichment in isoform 2 in the earliest (acidic) fractions. Enriched isoform 1 fraction, "B", and enriched isoform 2 fraction, "A", were selected for further purification.

Semipreparative Fractionation of IgG2 Structural Isoform 1. Isoform 1, from fraction "B", the basic portion of the preparative CEX profile, was buffer exchanged, concentrated, and further purified on a WCX-10 semiprep CEX column. Following fractionation of multiple injections, material was pooled based on elution profile. The pooled material was concentrated and buffer exchanged into formulation buffer. The final purity of purified material enriched in isoform 1 was evaluated by analytical CEX (Supporting Information Figure S1) and nonreduced CE-SDS (Figure 4A). The final

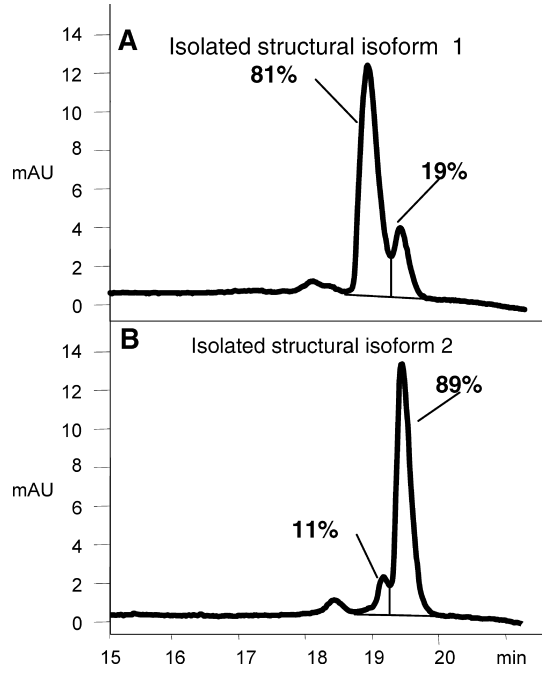

FIGURE 4: nrCE-SDS of CEX-purified structural isoforms. Structural isoforms 1 and 2 were isolated by CEX chromatography (Supporting Information Figure S1). (A) The final material enriched in isoform 1 had a CE-SDS ratio of isoform 1 to isoform 2 of 81%:19%. (B) The final material enriched in CE-SDS isoform 2 had a CE-SDS ratio of 11%:89%.

material enriched in isoform peak 1 showed a nrCE-SDS ratio of isoform peak 1 to isoform peak 2 of 81:19.

Semipreparative Fractionation of IgG2 Structural Isoform 2. Isoform 2 was enriched from fraction "A", the acidic portion of the preparative CEX profile. Reinjection of this preparative fraction onto analytical CEX showed a mixture of acidic variant and main CEX peak 1. Preparative CEX fraction "A" was buffer exchanged into 20 mM MES, pH 6, and concentrated. The acidic and main peak species were separated using a pH gradient. Fractions were pooled based on elution profile, then concentrated, and buffer exchanged into formulation buffer. The final purity of the pool was evaluated by analytical CEX (Supporting Information Figure S1) and nonreduced CE-SDS (Figure 4B). The final material enriched in isoform peak 2 showed a nrCE-SDS ratio of isoform peak 1 to isoform peak 2 of 11:89.

The potency of the purified isoforms was measured using an *in vitro* gene expression bioassay. Each isoform had comparable potency. This result indicates that the presence of structural isoforms does not influence antigen binding for this molecule. Analysis of both purified isoforms by ESI-TOF mass spectrometry (*14*) resolved three major glycosylated forms in each fraction, due to the presence of biantennary glycan structures on the C_H2 domain, consistent with the expected glycosylation pattern of antibodies (*18*). On the heavy chain, the two biantennary glycans ending with 0 galactose (0 Gal, G0) or 1 Gal (G1) are the major forms (approximately 40% each). The form with 2 Gal (G2) is minor. On the intact IgG2 molecule, a combination of two HC generate the major glycoforms with 0, 1, 2, and 3 Gal we reported in Supporting Information Table S1. Other glycoforms exist but in minor amounts. The results show that experimental masses of both fractions of purified isoforms are comparable and corroborate the expected primary structure $(HC\text{-}LC)_2$ (Supporting Information Table S1). The data further imply that the difference between the isoforms is structure-related.

Nonreduced Peptide Mapping. To better understand the structural differences between the isoforms, the disulfide structure of IgG2 (as an isoform mixture) was investigated by nonreduced peptide mapping. The potential presence of free cysteines in IgG2 could generate artifactual results linked to disulfide scrambling. A classic approach to eliminate this undesired side reaction is to alkylate free cysteine with *N*-ethylmaleimide (NEM) at acidic pH (*19*). After NEM alkylation, the solution was buffer exchanged, and an enzymatic digest was performed on the nonreduced molecule. Disulfide pair assignments were made by identification of bridged peptides using mass analysis (Figure 5A).

Cleavage of the nonreduced protein by trypsin generated several peptides which contained only one cysteine residue and were joined to form seven disulfide-linked fragments (peaks 1−7, Figure 5A). The identified IgG2 disulfide linkages are as follows (Table 1). For HC: Cys-22 to Cys-97; Cys-146 to Cys-202; Cys-259 to Cys-319; Cys-365 to Cys-423 (equivalent to HC positions 22, 92, 142, 208, 274, 340, 390, and 456 in Kabat numbering (*7*)). For LC: Cys-23 to Cys-88; Cys-134 to Cys-194 (same LC positions in Kabat numbering). For interchains: HC Cys-133 to LC Cys-214 (equivalent to positions HC 127 and LC 214 in Kabat numbering). These disulfide bonds correspond to interchain connectivity and to intrachain loops V_H, C_H1, C_H2, C_H3, V_L, and C_L of human IgG2 modeled from the X-ray crystallography structure of IgG1 (*4*). These experimental results provide evidence that the recombinant molecule has the expected human IgG2 disulfide bonds in these regions of the molecule.

Mass measurements of IgG2 tryptic peptides were then examined to further elucidate hinge region structures. Mass data showed that the hinge region was found, though at low levels, as a dimer of peptide 221 to 246 (peptide H_{16}) with four cysteine bridges in total formed between Cys-221, Cys-222, Cys-225, and Cys-228 (equivalent to HC positions 232, 233, 239, and 242 in Kabat numbering). This structure corresponds to the previously described human IgG2 hinge region (*11*). When the tryptic digest was reduced and alkylated, however, the fragment H_{16} recovery was as expected. This result suggests that the digest of the nonreduced molecule generated the expected fragment but only a fraction eluted as a conventional dimer. The linearly connected form of hinge dimer was quantified by single ion monitoring of peptides, generated by the nonreduced tryptic peptide map and compared with the monomer hinge peptides that were fully recovered from the reduced tryptic peptide map. The conventional hinge dimer was found to represent only 15% to 20% of the total hinge content. Analysis by mass spectrometry showed that the additional hinge fractions contained tryptic peptide H_{16} (hinge) covalently linked to peptides H_{10} (HC) and L_{18} (LC) (peak 8, Figure 5A, and peaks 8a−h, Figure 6A). The sequences of these peptides are depicted in Figure 7E. Based on the expected structure, however, peptides H_{10} and L_{18} would instead form only the interchain connection C_H1-C_L. These results obtained indicate the presence of a more complex structure of disulfide-linked fragments involving (hinge:HC:LC) complexes.

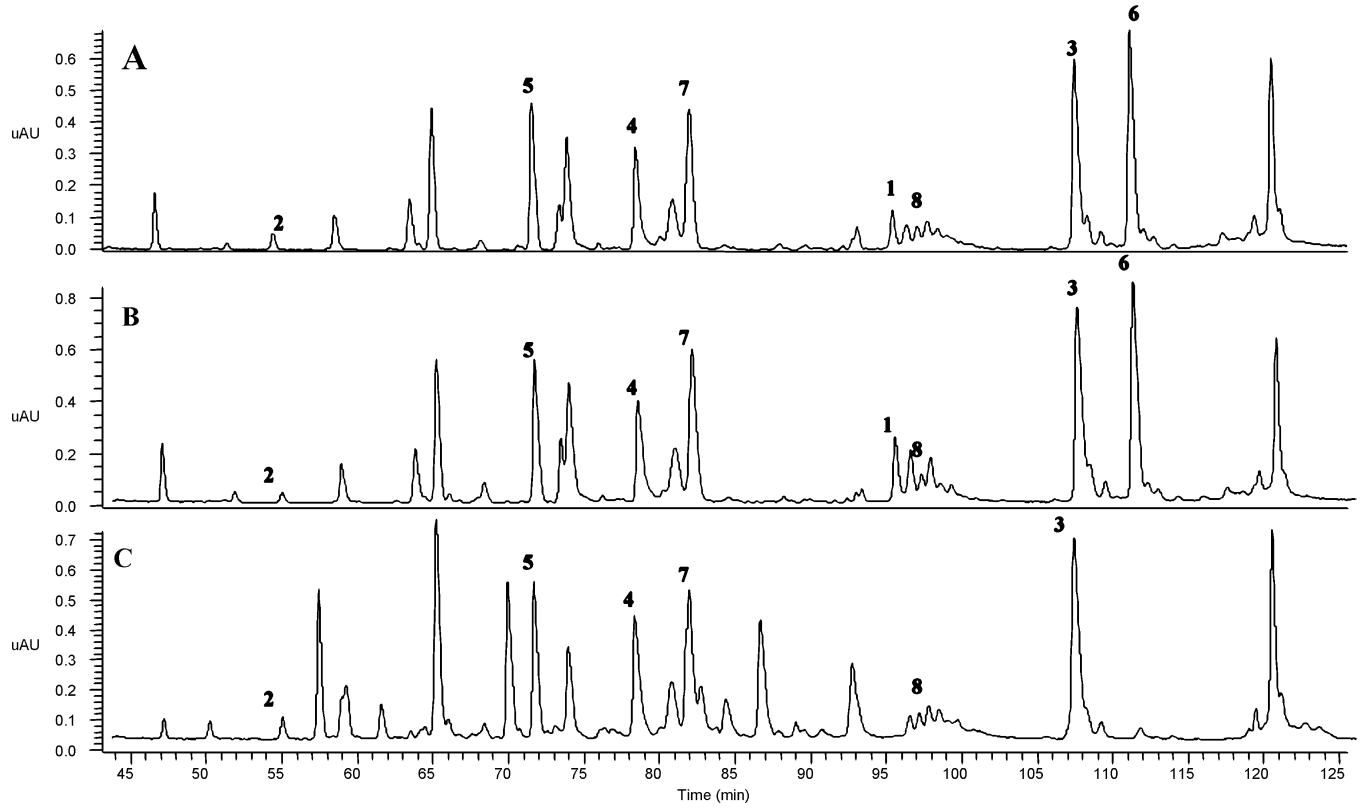

FIGURE 5: Identification of disulfide-bridged peptides using trypsin peptide mapping of the nonreduced molecule. (A) IgG2 reference. The labeled peaks represent the disulfide-linked tryptic peptides, and their corresponding masses are described in Table 1. The hinge complex disulfide-linked peptides elute at 95−100 min. (B) IgG2 reference treated by cysteine−cystine redox potential. The treatment modifies the hinge complex disulfide-linked peptides while maintaining the other disulfide-linked pairs. (C) Commercially available IgG2 isolated form serum of myeloma patients (Sigma). The hinge complex disulfide-linked peptides are visible in the same 95−100 min region. All of the disulfide-linked peptides that belong to constant regions can be identified by similarity to the IgG2 reference.

Table 1: Disulfide-Linked Heteropeptides: Assignments from Nonreduced Trypsin Digest[a]

				mass (Da)	
disulfide-linked fragments	residues	linkages	domain	theoretical	exptl
1	(H)1−40:(H)84−99	(H)Cys22−(H)Cys97	V_H	6031.7	6031.4
2	(H)124−135:(L)212−214	(H)Cys133−(L)Cys214	C_H1, C_L	1535.7	1535.8
3	(H)136−149:(H)150−212	(H)Cys146−(H)Cys202	C_H1	8073.9	8074.1
4	(H)254−286:(H)319−320	(H)Cys259−(H)Cys319	C_H2	3986.8	3989.6
5	(H)359−368:(H)415−437	(H)Cys365−(H)Cys423	C_H3	3847.4	3847.5
6	(L)19−42:(L)62−103	(L)Cys23−(L)Cys88	V_L	7270.0	7270.5
7	(L)127−142:(L)191−207	(L)Cys134−(L)Cys194	C_L	3558.1	3558.5
8f $(H_{15-16})_2$	(H)220−246:(H)220−246	(H)Cys221−(H)Cys221	hinge	5610.9	5610.3
8h $(H_{16})_2$	(H)221−246:(H)221−246	(H)Cys222−(H)Cys222	hinge	5354.6	5356.7
8g $(H_{15-16}{:}H_{16})$	(H)221−246:(H)221−246	(H)Cys225−(H)Cys225 (H)Cys228−(H)Cys228	hinge	5482.6	5480.9
8e $H_{10}{:}(H_{16})_2{:}L_{18}$	(H)221−246		hinge, C_H1, C_L	6892.3	6889.4
8c $H_{10}{:}(H_{15-16})_2{:}L_{18}$	(H)220−246		hinge, C_H1, C_L	7148.3	7145.9
8d $H_{10}{:}(H_{15-16}{:}_{16}){:}L_{18}$	(H)124−135		hinge, C_H1, C_L	7020.3	7016.4
8a $(H_{10})_2{:}(H_{15-16})_2{:}(L_{18})_2$	(L)212−214		hinge, C_H1, C_L	8682.1	8680.4
8b $(H_{10})_2{:}(H_{15-16}{:}_{16}){:}(L_{18})_2$			hinge, C_H1, C_L	8554.1	8550.4

[a] The disulfide-linked fragments are tabulated according to the peak labels shown in Figures 5 and 6. (H), heavy chain peptides; (L), light chain peptides.

As described previously, analysis by nrCE-SDS shows that application of a redox potential modified the structural isoforms, resulting in a significant decrease of peak 1 (40% to 12%) concomitant with an increase of peak 2 (60% to 88%). To learn more about the hinge structures generated by redox treatment, the disulfide structure of the resulting material was investigated by the same nonreduced trypsin procedure (Figure 5B and Table 1). Mass spectrometric analysis of the disulfide-linked peptides showed that most peptides were of the symmetrical form $(H_{10})_2-(H_{16})_2-(L_{18})_2$, corresponding to the hinge dimer covalently linked to both heavy chain and light chain (Table 1). No linearly connected hinge dimer was observed. We conclude that application of a cysteine:cystine redox potential, a procedure that should lead to the thermodynamically most stable isoform, favors the structure corresponding to structural isoform 2, i.e., which is devoid of molecules containing the conventional linearly paired hinge peptides.

A similar nonreduced peptide map analysis was performed on commercially available IgG2 isolated from myeloma

Table 2: Mass Measurement of Disulfide-Linked Peptides from Tryptic Digest of Nonreduced Human IgG2 Isolated from Serum of Myeloma Patients[a]

disulfide-linked peptides	domain	mass (Da)	
		theoretical	exptl
2	C_H1, C_L	1535.7	1535.7
3	C_H1	8073.9	8073.1
4	C_H2	3986.8	3989.0
5	C_H3	3847.4	3847.5
7	C_L	3558.1	3557.7
8e H_{10}:$(H_{16})_2$:L_{18}	hinge, C_H1, C_L	6892.3	6889.2
8c H_{10}:$(H_{15-16})_2$:L_{18}	hinge, C_H1, C_L	7148.3	7147.4
8d H_{10}:$(H_{15-16}$:$_{16})$:L_{18}	hinge, C_H1, C_L	7020.3	7017.8
8a $(H_{10})_2$:$(H_{15-16})_2$:$(L_{18})_2$	hinge, C_H1, C_L	8682.1	8681.5
8b $(H_{10})_2$:$(H_{15-16}$:$_{16})$:$(L_{18})_2$	hinge, C_H1, C_L	8554.1	8552.2

[a] The disulfide-linked peptides are tabulated according to the peak labels described in Figures 5C and 6B. The mass measurements are interpreted by analogy with the recombinant IgG2 sequence.

(Figures 5C−6B). Although the complete primary sequence of these molecules is not known, sequence homology within the constant regions allows to conclude that disulfide-linked fragments involving (hinge:HC:LC) complexes (peak 8, Figure 5C; peaks 8a−f, Figure 6B and Tables 1 and 2) are identical.

Isolation of Disulfide-Linked Heteropeptides. We developed a preparative method to resolve the disulfide-linked heteropeptides present in peaks 1 and 2 to further reveal the structural differences in each isoform. A method combining chemical and enzymatic cleavage with size exclusion chromatography under denaturing conditions (dSEC) was developed to purify preparative amounts of disulfide-linked peptides. To minimize the possibility of disulfide scrambling, reactive cysteines were blocked by treatment with the alkylating reagent, NEM, at acidic pH (*19*). This prevents disulfide bond exchange and facilitates characterization of bridged residues. The next step simplified the analysis by reducing the size of the antibody to a section containing the disulfide-linked fragments. Treatment of IgG2 with cyanogen bromide (CNBr) cleaved the light chain at a single methionine residue at Met-4 and the heavy chain at Met-114, Met-250, Met-356, Met-395, and Met-426. Cleavage by CNBr reduced the complexity of the analysis by reducing the size of the molecule from 150 kDa to a 75 kDa fragment containing covalently linked C_L, V_L, C_H1, and hinge. Trypsin digestion further reduced the size of the disulfide-linked peptides as shown in Supporting Information Figure S2. Purified structural isoforms 1 and 2 were treated according to the CNBr/trypsin procedure, and the resulting digests were separated by dSEC into six peaks, A−F. The dSEC profiles of isoforms 1 and 2 are shown in Figure 7A. The disulfide-linked peptides separated in dSEC fractions were identified by RP-HPLC-MS (Figure 7B-D) and are presented in Table 3.

Several disulfide-linked peptides, nonrelated to the hinge region, were identified. The disulfide-linked fragment H_{11}:H_{12} (8074 Da) was found in dSEC peak B. The disulfide-linked fragments L_2:L_5 (7271 Da) and L_9:L_{16} (3559 Da) were identified in dSEC fractions C and D, respectively. From these data, the cysteine residue linkages were deduced as (HC) Cys-146 to (HC) Cys-202, (LC) Cys-23 to (LC) Cys-88, and (LC) Cys-134 to (LC) Cys-194. These disulfide bond linkages are consistent with the results obtained by nonreduced peptide mapping (Table 1) and correspond to intrachain loops C_H1, V_L, and C_L of human IgG2 modeled from the crystal structure.

We focused the analysis on heteropeptides containing the hinge region. Mass measurement showed that in the dSEC profiles of each isoform 1 and 2 (Figure 7A) the disulfide-linked (hinge:HC:LC) peptides were contained in fractions B and C. We isolated these complexes and determined their precise cysteine connectivity as detailed below.

Analysis of Disulfide Linkages by Partial Reduction/Alkylation. A partial reduction/alkylation technique, derived from the methods developed to solve the structure of proteins with cystine knot domains (*19, 20*), was used to determine the disulfide linkages. The connection between the cysteine residues were characterized using partial reduction at acidic pH with tris(2-carboxyethyl)phosphine hydrochloride (TCEP), followed by alkylation at acidic pH with NEM (*19*). This procedure controls the specific release of a limited number of disulfide bridges and results in a mixture of heteropeptides with different amounts of reduced/alkylated cysteine residues. Partially reduced heteropeptides were then treated by iodoacetic acid (IAA), resulting in IAA-modified cysteine residues that can be distinguished from NEM-tagged cysteine residues based on mass. N-Terminal sequencing and MS/MS sequencing were performed to locate the NEM tag on open cysteine pairs and to elucidate the disulfide linkages present prior to partial reduction/alkylation treatment.

Disulfide-Linked Peptides Identified in Structural Isoform 1. Investigation of isoform 1 was carried out first. RP-HPLC-MS analysis was used to separate the disulfide-linked peptides obtained in the dSEC fractions.

Structural Isoform 1. Symmetrical Complex in dSEC Fraction C. Mass measurement of dSEC fraction C of isoform 1 (Figure 7A) resulted in three masses (5352, 5481, and 5608 Da) interpreted as hinge dimer $(H_{16})_2$, $(H_{15-16}$:$H_{16})$, and $(H_{15-16})_2$, respectively (Figure 7C, Table 3). Some heterogeneity was observed in the cleavage of the hinge regions at Arg-219/Lys-220 that resulted in the generation of H_{15-16} and H_{16} peptides. Complete analysis of the cysteine connectivity in the hinge dimer is described in Supporting Information. The results show that when the hinge was present as a dimer free of disulfide linkage to any constant domain (15−20% of IgG2 molecules), the four disulfides are connected in parallel as interchain bridges of the form (HC) Cys-221 to (HC) Cys-221, (HC) Cys-222 to (HC) Cys-222, (HC) Cys-225 to (HC) Cys-225, and (HC) Cys-228 to (HC) Cys-228. These cysteine connections are consistent with the IgG2 structure described in the literature (*11*). This structure is defined by a structurally independent hinge covalently linked by parallel disulfide bonds and the Fab interchain connection between V_L and C_H1 (Cys-214 to Cys-133). The schematic representation of the symmetrical structural isoform present in CE peak 1, we denote IgG2-A, is shown in Figure 8 (top left).

Structural Isoform 1. Asymmetrical Complex in dSEC Fraction B. Analysis of the heterogeneous disulfide-linked peptides isolated from fraction B of the dSEC trace of structural isoform 1 by RP-HPLC (Figure 7B) resulted in three major masses (7146, 7016, and 6889 Da) interpreted as a complex resulting from the connection of a hinge dimer with heavy chain fragment H_{10} and light chain fragment L_{18} (Table 3). As described above, the presence of three masses for the same complex was due to some cleavage heterogeneity at Arg-219/Lys-220 that resulted in the generation of H_{15-16} and H_{16} peptides. The proposed complex is an

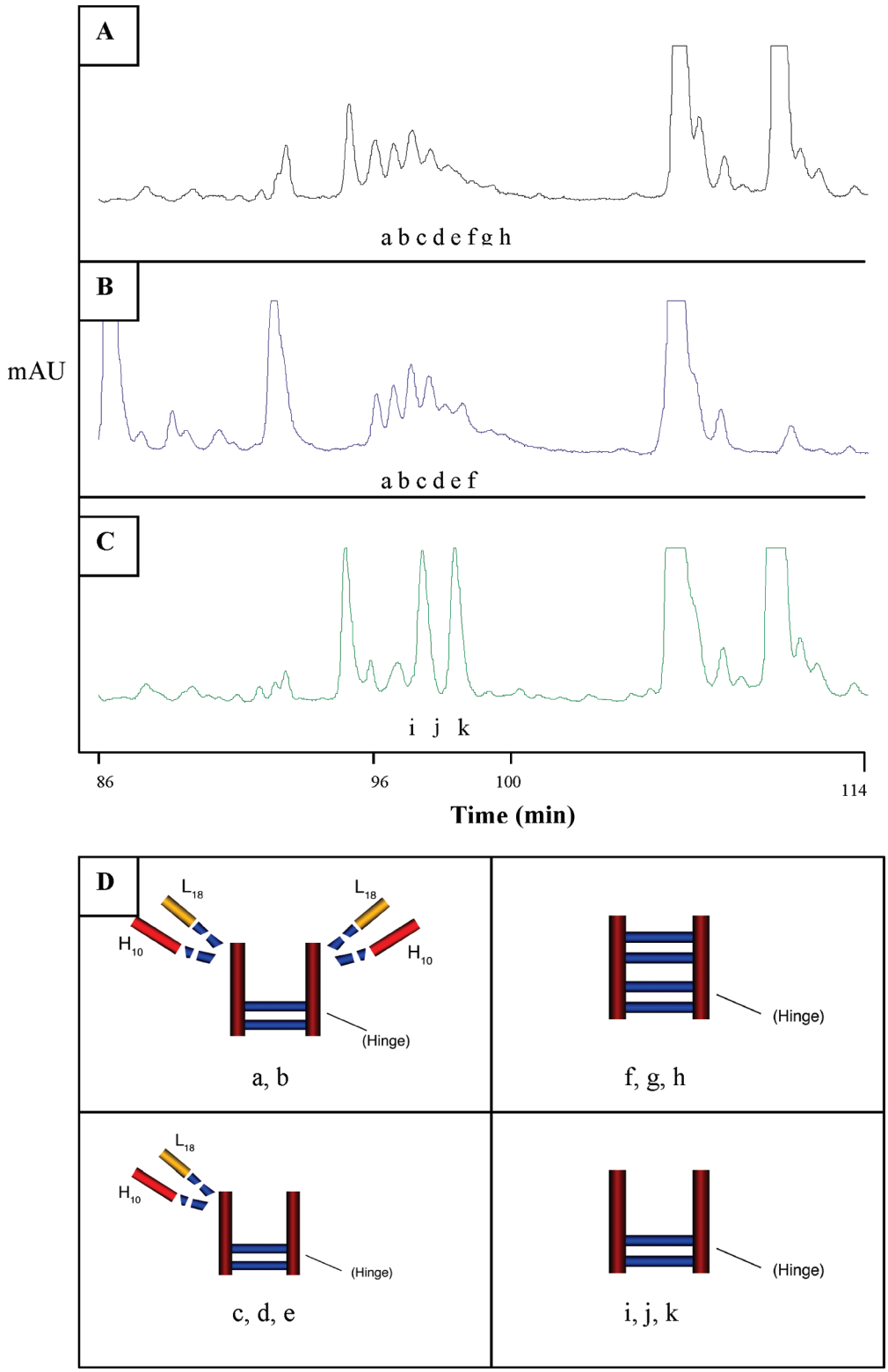

FIGURE 6: LC-MS analysis of disulfide-linked heteropeptides. This figure shows an expanded view of Figure 5 focused of the hinge disulfide-linked complexes eluting at 95−100 min (peak 8). The tryptic peptide representing the hinge region, H_{16} (or H_{15-16}), is found covalently bound to the tryptic peptides H_{10} and L_{18}, normally involved in the interchain connection C_H1-C_L. (A) Trypsin peptide mapping of nonreduced IgG2 reference material. Different arrangements of the four peptides, labeled 8a−h, are separated by LC-MS. (B) Tryptic peptide mapping on nonreduced commercially available IgG2 isolated from serum of myeloma patients shows a distribution of hinge complex peptides similar to IgG2. (C) IgG2 which has been mutated at C221 and/or C222 does not show these hinge complex disulfide-linked peptides but rather exhibits full recovery of the expected linearly paired hinge region. These peptides, labeled 8i−k, are 221/222 C−S hinge dimers, different by one residue from the IgG2 hinge dimers 8f−h. (D) Schematic representation of the hinge complex disulfide-linked peptides for these IgG2 molecules. 8a−b = peptides $(H_{10})_2-$hinge$-(L_{18})_2$; 8c−e = peptides $(H_{10})-$hinge$-(L_{18})$; 8j−h = hinge peptides $(H_{15-16})_2$, $(H_{16}{:}H_{15-16})$, and $(H_{16})_2$. The masses of the hinge complex peptides 8a−h are presented in Table 1.

asymmetrical arrangement of the form $[H_{10}-(\text{hinge})_2-L_{18}]$ schematically represented in the inset of Figure 7A.

Partial reduction/alkylation treatment of dSEC fraction B (7146 Da) generated two groups of peaks. One was H_{10},

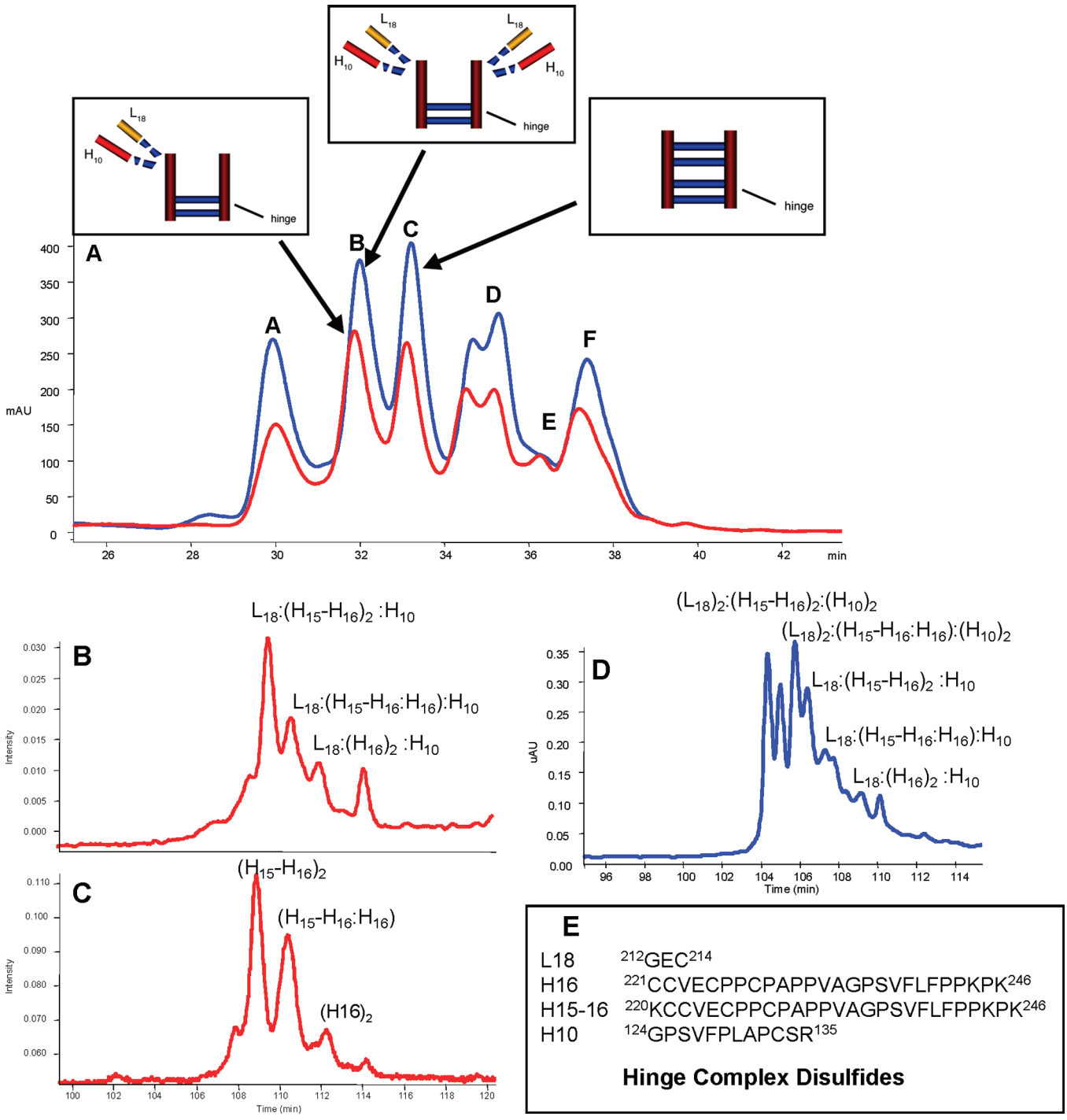

FIGURE 7: Separation by dSEC of CNBr/tryptic disulfide-linked complexes. (A) dSEC of CNBr/tryptic peptides generated from purified isoform 1 (red trace) and isoform 2 (blue trace). (B−D) LC-MS of the heterologous disulfide-linked peptides. (B) LC-MS of dSEC fraction B, isolated from isoform 1, gave three major masses interpreted as a complex resulting from the connection of H_{10} and L_{18} with a hinge dimer, either $(H_{16})_2$ or $(H_{15-16}{:}H_{16})$ or $(H_{15-16})_2$. (C) LC-MS of dSEC fraction C, isolated from isoform 1, gave three masses interpreted as hinge dimer, $(H_{16})_2$, $(H_{15-16}{:}H_{16})$, and $(H_{15-16})_2$, respectively. (D) LC-MS of dSEC fraction B, isolated from isoform 2, shows that the heterologous peptides represent a mixture of symmetrical and asymmetrical complexes of the forms $[(H_{10})_2{-}(\text{hinge})_2{-}(L_{18})_2]$ and $[H_{10}{-}(\text{hinge})_2{-}L_{18}]$. The symmetrical complexes elute first (104−106 min) followed by the asymmetrical complexes (106−110 min). LC-MS of dSEC fraction C, isolated from isoform 2, indicated that no hinge dimer was present in isoform 2 (not shown). (E) Sequences of the disulfide-linked heteropeptides, hinge peptides (H_{15-16}, H_{16}), HC fragment H_{10}, and LC fragment L_{18}.

carrying a NEM-alkylated cysteine, which eluted at 46 min, and the other was a group of major peptides, with masses of 6041 and 5914 Da, that were interpreted as a complex of $[\text{NEM}{-}(\text{hinge})_2{-}L_{18}]$ (Supporting Information Figure S3A). This result shows that upon partial reduction the original disulfide complex lost peptide H_{10}. The two disulfide-linked peptides, 6041 and 5914 Da, were completely reduced and alkylated with IAA (Supporting Information Figure S3B). The major alkylated product measured 3040 Da and was interpreted as the hinge monomer H_{15-16} with four residues modified by IAA. The other major peak, 3107 Da, is the hinge monomer H_{15-16} with three cysteine residues modified by IAA and 1 NEM-labeled cysteine. N-Terminal sequencing of alkylated peptide 3107 Da shows that the NEM modifica-

Table 3: Measured Masses of Disulfide-Linked Peptides Separated by dSEC[a]

disulfide-linked tryptic fragments	dSEC fractions	amino acid residues	mass (Da) theoretical	mass (Da) exptl
trypsin	fraction A		23463.5	23462.4
trypsin fragment				17515.7
H_{11}:H_{12}	fraction B	(H)136−149:(H)150−212	8074.9	8073.8
H_{11}:H_{12p}		(H)136−149:(H)162−212	6638.3	6638.0
H_{10}:$(H_{16})_2$:L_{18}	fraction B	(H)124−135:[(H)221−246]$_2$:(L)212−214	6891.3	6889.4
H_{10}:$(H_{15-16})_2$:L_{18}		(H)124−135:[(H) 220−246]$_2$:(L)212−214	7147.3	7145.9
H_{10}:$(H_{15-16:16})$:L_{18}		(H)124−135:[(H)221−246:(H)221−246:(L)212−214	7019.5	7016.4
$(H_{10})_2$:$(H_{15-16})_2$:$(L_{18})_2$		[(H)124−135]$_2$:[(H)220−246]$_2$:[(L)212−214]$_2$	8682.1	8680.4
$(H_{10})_2$:$(H_{15-16:16})$:$(L_{18})_2$		[(H)124−135]$_2$:(H)220−246:(H)221−246:[(L)212−214]$_2$	8554.1	8550.4
L_2:L_5	fraction C	(L)19−42:(L)62−103	7271.0	7271.2
$(H_{16})_2$	fraction C	[(H)221−246]$_2$	5355.6	5352.2
$(H_{15-16})_2$		[(H)220−246]$_2$	5611.6	5608.4
$(H_{15-16}$:$H_{16})$		(H)220−246:(H)221−246	5483.6	5480.9
L_9:L_{16}	fraction D	(L)127−142:(L)191−207	3559.1	3558.5

[a] The dSEC profiles for isoform 1 (red trace) and isoform 2 (blue trace) are shown in Figure 7. The hinge dimer is found in fraction C; the hinge-containing disulfide-linked peptides are found in fraction B.

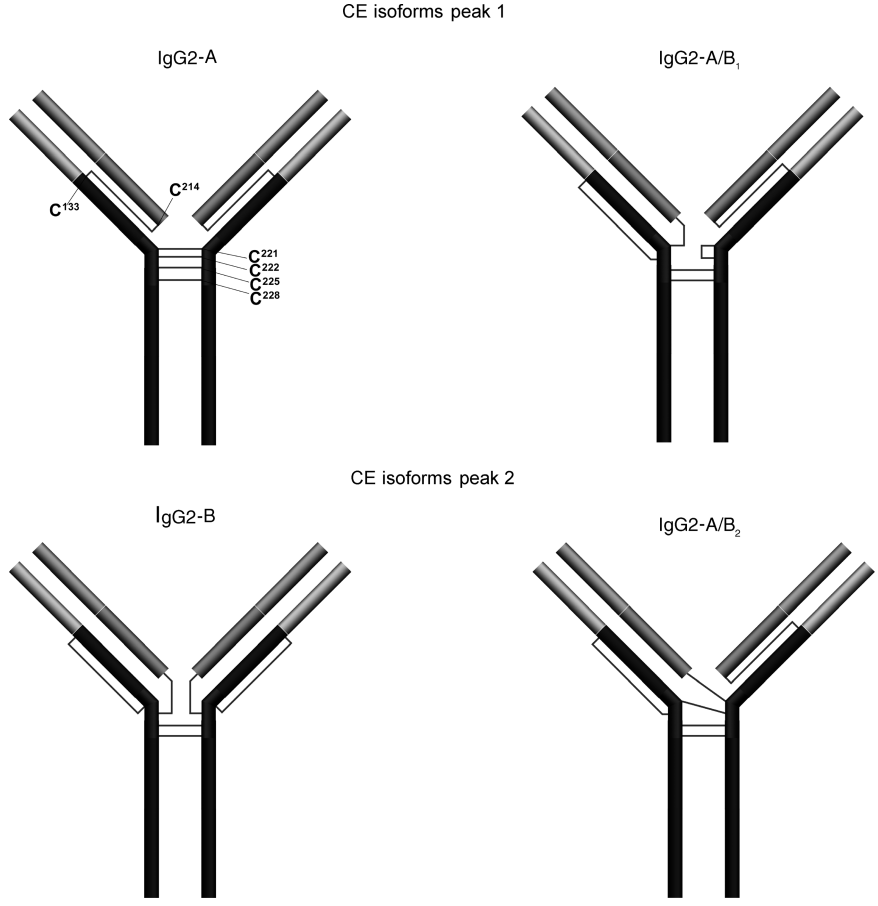

FIGURE 8: Disulfide linkages and schematic representation of structural isoforms on IgG2 models. Analysis of the connectivity of cysteine residues defines four molecules with symmetrical (A, B) or asymmetrical (A/B) disulfide linkages. The symmetrical form IgG2-A is the structure described in the literature. In the symmetrical form IgG2-B, the disulfide linkages are equivalent on the two sides of the molecule, with both HC and LC covalently linked to the hinge. In the asymmetrical forms (A/B_1, A/B_2), only one side displays the classical HC133−LC214 linkage (of IgG2-A), whereas the other side exhibits LC−hinge and HC−hinge covalent linkages (as in IgG2-B).

tion is found on the (HC) Cys-222. This result demonstrates that in the asymmetrical complex in isoform 1, (HC) Cys-133 (peptide H_{10}) was originally linked to the hinge region through a connection with (HC) Cys-222. Complete alkylation of H_{15-16} with four IAA (3040 Da) shows that a major portion of the hinge peptide has no connection with either H_{10} or L_{18} in the original structure. This result suggests that in the asymmetrical complex the opposite side of the hinge has intrachain disulfide bridges of the form (HC) Cys-221 linked to vicinal (HC) Cys-222. The interchain C_H1-C_L is formed by the classic disulfide (HC) Cys-133 to (LC) Cys-214. A schematic representation of the asymmetrical structural isoform present in CE peak 1 is shown in Figure 8 (top right).

Disulfide-Linked Peptides Identified in Structural Isoform 2. In-depth analysis of isoform 2 was then carried out. The dSEC profile of isoform 2 following the CNBr/trypsin digestion procedure is shown in Figure 7A (blue trace).

Structural Isoform 2, dSEC Fraction C. RP-HPLC-MS analysis of dSEC fraction C from purified isoform 2 showed that no conventional hinge dimer was present. A structurally isolated hinge region does not exist in isoform 2.

Structural Isoform 2. Complexes Found in dSEC Fraction B. Mass measurement of RP-HPLC separated peptides from dSEC fraction B, from isoform 2, shows that the heterologous peptides represent a mixture of symmetrical and asymmetrical complexes. The symmetrical complexes at 8550 and 8680 Da (Figure 7D, Table 1) representing the form $[(H_{10})_2-(hinge)_2-(L_{18})_2]$ were analyzed by partial reduction/alkylation with NEM. LC-MS analysis showed that a distribution of unaffected starting material, at 8680 Da, and partially alkylated peptides, with major masses measured at 8324, 8367, and 7,268 Da, was obtained (Supporting Information Figure S4A). These products were isolated and completely reduced with DTT, alkylated with IAA an analyzed by LC-MS. Complete IAA alkylation of the 8324 Da disulfide-linked peptide, interpreted as the $[(H_{10})_2-(hinge)_2-(NEM)_2]$ complex, which lost two L_{18} peptides upon partial reduction, is shown in Supporting Information Figure S4B. Mass analysis showed that the major product, 3107 Da, was interpreted as the hinge peptide carrying four alkylated cysteines. Of the four alkylated cysteines, three were modified by IAA and one was modified by NEM. N-Terminal sequencing of peptide 3107 Da identified the NEM label on (HC) Cys-222 (Supporting Information Figure S4B). This result indicates that in the symmetrical component of isoform 2, (LC) Cys-214 (peptide L_{18}), was originally linked to the hinge region through a connection with (HC) Cys-222.

Analysis of the alternative form obtained by partial reduction, 8367 Da, interpreted as $[(H_{10})_2-(hinge)_2-L_{18}-NEM]$, the form which only lost a single L18 peptide, confirms the presence of NEM on (HC) Cys-222. Therefore, this demonstrated that the original connection of L_{18} is to (HC) Cys-222. The last partially reduced form, 7268 Da, which corresponds to the loss of both H_{10} and L_{18}, generating a complex $[(H_{10})-(hinge)_2-L_{18}-(NEM)_2]$, was recovered in minor amounts and did not lead to any further information. The symmetrical complex in isoform 2, we denote IgG2-B, is shown schematically in Figure 8 (bottom left).

The disulfide-linked peptides (6889, 7016, and 7146 Da) resulting from the asymmetrical component isolated from isoform 2, of the form $[H_{10}-(hinge)_2-L_{18}]$, are depicted in Figure 7A. Partial reduction of MW 7146 Da yielded two products with masses of 7398 and 7269 Da, consistent with the structure $[H_{10}-(hinge)_2-L_{18}-(NEM)_2]$ (Supporting Information Figure S5A). This result shows that partial reduction of isoform 2 does not release the peptides H_{10} and L_{18}, but rather opens a bond inside the hinge region. This result differs from that of asymmetrical isoform 1 of similar mass, which exhibited loss of L_{18} or H_{10} upon partial reduction, while the hinge disulfides remained intact. Complete reduction and alkylation of 7398 Da species (peak 1) and analysis by N-terminal sequencing indicate that the NEM label was present at positions Cys-221 and Cys-222, which corresponds to the original interconnection within the hinge region. The other mass resulting from the partial reduction is 7088 Da, which represents $[(H_{15-16}:H_{16})-(H_{10})-(NEM)_3]$. This mass represents a complex that lost L_{18} and had one hinge disulfide reduced (Supporting Information Figure S5B). This species was completely reduced with DTT and alkylated with IAA. N-Terminal sequencing of the alkylated peptide identified (HC) Cys-221 as the location of the NEM-labeled residue, which is consistent with the connection of L_{18} at position (HC) Cys-221. The facile partial reduction of hinge disulfides, while maintaining H_{10} and L_{18}, suggests a different structure than isoform 1. Complete alkylation of this product shows a hinge species that can only be attributed to an interconnection between Cys-221 and Cys-222. This interchain connection is concomitant with a connection of H_{10} to Cys-222 on one side of the hinge and L_{18} to Cys-221 on the other side of the hinge. A schematic representation of the asymmetrical complex in isoform 2 is shown in Figure 8 (bottom right).

In summary, determination of the disulfide connectivity of IgG2 structural isoforms defines four different structures, presented schematically in Figure 8. IgG2-A (top left) is the conventional model with Fab and hinge regions structurally independent. IgG2-B (bottom left) is a symmetrically arranged isoform with the two Fab arms covalently attached to the hinge by disulfide bridges. IgG2-A/B is an intermediate form with one Fab arm structurally independent of the hinge, as found in form A, and the other Fab arm covalently linked to the hinge, as found in form B. We describe two different structures of this type, denoted IgG2-A/B_1 (top right) and IgG2-A/B_2 (bottom right). These results show that human IgG2 molecules display unique disulfide connectivity pattern for each form.

Elimination of the Structural Isoforms by Mutation of a Single Cysteine. The data described above show evidence for the presence of different disulfide bond arrangements involving only four cysteines: the cysteine of the heavy chain located in C_H1, Cys-133, the cysteine at the C-terminus of the light chain, Cys-214, and two cysteines in the hinge region, specific to the IgG2 subclass, Cys-221 and Cys-222. The other two cysteines of the hinge region form an interchain linkage between Cys-225 of both heavy chains and Cys-228 of both heavy chains and are not involved in the different structural isoforms. Modeling of the IgG2 sequence based on three-dimensional antibody structure places the four cysteines in close spatial proximity (Figure 2), supporting the concept that a variable arrangement of these residues could generate IgG2 structural isoforms. We tested the possibility that mutation of the closely spaced cysteines could eliminate these forms. Two specific cysteine-to-serine mutants were prepared by site-directed mutagenesis at either position 221 or 222. Mutant proteins expressed from stably transfected chinese hamster ovary (CHO) cells were purified by protein A affinity chromatography and comparatively analyzed. Mutants C221S and C222S exhibited no significant difference in expression and purification characteristics when compared to wild-type IgG2. All three molecules had similar potency in reporter gene expression bioassay. However, when analyzed by nrCE-SDS and nonreduced peptide mapping, the molecules behaved differently. The mutant antibodies lost the typical IgG2 doublet and were resolved in a single peak by nrCE-SDS (Figure 3C). Furthermore, in contrast to the wild type, application of a redox potential had no impact on the electrophoretic profile of the mutant antibodies (Figure 3C). Nonreduced tryptic peptide mapping of the mutants showed quantitative recovery of the linearly connected hinge dimer and the

$H_{10}-L_{18}$ heteropeptide expected from the conventional interchain connection C_H1-C_L (Figure 6C). These results indicate that mutation of a single cysteine residue specifically abolishes the IgG2 structural isoforms and generates a homogeneous antibody structure.

DISCUSSION

Human IgG2s are distinguished from other isotypes by their preferential response toward polysaccharide antigens as well as their limited ability to engage Fc-mediated effector functions. From the analysis of this molecule, other recombinant IgG2 molecules expressed at Amgen, as well as natural human IgG2 molecules isolated from plasma (*12*), we present the concept of structural isoforms as a general feature of IgG2 molecules. In the case described here, these structural isoforms have similar antigen binding activity *in vitro*; however, we have also observed that certain IgG2/antigen complexes exhibit variable potency (13). The additional disulfide linkages between the hinge and Fab regions demonstrated in this study may restrict IgG2 structural flexibility. This is in agreement with electron microscopy studies of human IgG subclasses, showing that the order of flexibility in human hinges is IgG3 > IgG1 > IgG4 > IgG2 (*21*) and suggests that the IgG2 subclass represents a specific case among immunoglobulins.

Evolution has favored emergence of a hinge region in mammalian immunoglobulins for increased flexibility and the ability to adopt a large number of conformations in solution (*22, 23*), but in this context, IgG2 molecules appear clearly less flexible. Their more rigid structures could represent an early state of IgG development which is supported by the fact that the IgG2 subclass is the most evolutionary distant of all human immunoglobulins (*24*). In human immunoglobulins, the constant regions share >95% homology, whereas the hinge regions are significantly divergent, illustrating a high evolutionary pressure on this domain. Our results show that elimination of one of the two cysteine residues in the hinge region specific to the IgG2 subclass, Cys-221 or Cys-222, abolishes the structural isoforms and generates a homogeneous structure. We can speculate that elimination of these two cysteine residues during human evolution would result in an IgG1-like hinge, leading to simplification of the number of immunoglobulin structures, optimized flexibility of these molecules, and better adaptability of the immune response.

The presence of covalent IgG2 dimers in normal pooled human sera has been reported, and the authors attributed the dimer assembly to cross-linking of the hinge cysteines (*24*). Our report presents arguments for a dynamic exchange of IgG2 disulfide bridges between hinge, C_H1 and LC domains. The two results appear complementary. It is possible that *in vivo* disulfide exchange could happen, generating the covalent dimers described in Yoo et al. (*24*). Our system is different in the sense that we worked on purified recombinant antibodies expressed in CHO cells at large scale. We found that most of the material was secreted as monomer. Once purified, these IgG2 isoforms are stable as monomers. Upon storage, dimers are slowly formed, both noncovalent and covalent, but they stay at a very minor level.

The hinge structures specific to IgG2 that we have described may play a role in the specialization of this subclass, notably the preferential response toward polysaccharide antigens and the limited ability to initiate Fc-mediated effector functions. Yoo et al. (*24*) discussed lines of evidence suggesting that isotypes involved in the anticarbohydrate response contain unique features not present in other IgGs. Furthermore, the molecular basis explaining the limited ability of the IgG2 molecules to engage Fc-mediated effector functions is not totally clear. Specificity of the primary sequence has been suggested, and notably residues of the lower hinge region (residues 247−250, Kabat numbering), totally conserved in IgG1, 3 and 4 isotypes but different for IgG2, have been shown to be crucial for effector functions (*25*). However conflicting results have been reported. Whereas mutation experiments involving incorporation of IgG2 lower hinge residues into IgG1 or IgG3 sequences reduced or abolished binding, *in vitro* experiments using synthetic peptides mimicking these regions showed equivalent affinity in the context of either IgG1 or IgG2 lower hinges (*26–28*). These results suggest that, in addition to primary sequence, structural conformation may play a role in the limited ability of IgG2 to trigger effector functions. It is known that some effector functions are mediated through specific interactions with the hinge proximal region of CH2. While the specific three-dimensional arrangement of the isoforms described here is not known, it is possible that covalent bonding between the hinge and C_L or C_H1 could alter the overall folding of the molecule in such a way as to sterically restrict access to the hinge proximal residues in CH2. This may partially explain the limited effector functions associated with human IgG2. As this deficiency appears to be overcome above a certain concentration threshold (*29*) and IgG2 has been shown to be able to engage a certain allotype of FcγRIIa (*25*), it would be interesting to look at the specific response of purified structural isoforms to evaluate whether part of the population of IgG2s has normal interaction similar to other IgGs. Taken together, these facts illustrate the unique complexity of the IgG2 subclass. The presence of alternative IgG2 structural forms could explain some of the biological responses attributed only to the IgG2 immunoglobulin family. More studies are warranted to build on the discovery of these isoforms and address their biological significance *in vivo*.

ACKNOWLEDGMENT

We thank Jette Wypych, Greg Flynn, Pavel Bondarenko, Margaret Ricci, and Tom Dillon for helpful discussions. We also thank Dean Pettit and Jim Thomas for their support.

SUPPORTING INFORMATION AVAILABLE

Analysis of the disulfide connectivity of the hinge dimer, one table, and five figures. This material is available free of charge via the Internet at http://pubs.acs.org.

NOTE ADDED AFTER ASAP PUBLICATION

This paper published ASAP on June 13, 2008 with errors in both the Results and Discussion Sections. The correct version was published on June 19, 2008.

REFERENCES

1. Poljak, R. J., Amzel, L. M., Chen, B. L., Phizakerley, R. P., and Saul, F. (1974) The three-dimensional structure of the Fab′ fragment

of a human myeloma immunoglobulin at 2.0 angstrom resolution. *Proc. Natl. Acad. Sci. U.S.A. 71*, 3440–3444.
2. Deisenhofer, J. (1981) Crystallographic refinement and atomic models of a human Fc fragment and its complex with fragment B of protein A from *Staphylococcus aureus* at 2.9 and 2.8 angstrom resolution. *Biochemistry 20*, 2361–2370.
3. Davies, D. R., and Chacko, S. (1993) Antibody structure. *Acc. Chem. Res. 26*, 421–427.
4. Padlan, E. A. (1996) X-ray crystallography of antibodies. *Adv. Protein Chem. 49*, 57–133.
5. Aalberse, R. C., and Schuurman, J. (2002) IgG4 breaking the rules. *Immunology 105*, 9–19.
6. van der Neut Kolfschoten, M., Schuurman, J., Losen, M., Bleeker, W. K., Martinez, P., Vermeulen, E., den Bleker, T. H., Wiegman, L., Vinck, T., Aarden, L. A., de Bates, M. H., van de Winkel, J. G., Aalberse, R. C., and Parren, P. W. (2007) Anti-inflammatory activity of human IgG4 antibodies by dynamic Fab arm exchange. *Science 317*, 1554–1557.
7. Kabat, E. A., Wu, E. A., Perry, T. T., Gottesman, H. M. K. S., and Foeller, C. (1991) in *Sequences of Proteins of Immunological Interest*, 5th ed., U.S. Public Health Service, NIH, Washington, DC.
8. Harris, L. J., Larson, S. B., Hasel, K. W., and McPherson, A. (1997) Refined structure of an intact IgG2a monoclonal antibody. *Biochemistry 36*, 1581–1597.
9. Harris, L. J., Skaletsky, E., and McPherson, A. (1998) Crystallographic structure of an intact IgG1 monoclonal antibody. *J. Mol. Biol. 275*, 861–872.
10. Saphire, E. O., Stanfield, R. L., Crispin, M. D. M., Parren, P. W. H. I., Rudd, P. M., Dwek, R. A., Burton, D. R., and Wilson, I. A. (2002) Contrasting IgG structures reveal extreme asymmetry and flexibility. *J. Mol. Biol. 319*, 9–18.
11. Milstein, C., and Frangione, B. (1971) Disulphide bridges of the heavy chain of human immunoglobulin G2. *Biochem. J. 121*, 217–225.
12. Wypych, J., Li, M., Guo, A., Zhang, Z., Martinez, T., Allen, M. J., Fodor, S., Kelner, D. N., Flynn, G. C., Liu, Y. D., Bondarenko, P. V., Speed Ricci, M., Dillon, T. M., and Balland, A. (2008) Human IgG2 antibodies display disulfide mediated structural isoforms, *J. Biol. Chem.* . (published online).
13. Dillon, T. M., Speed Ricci, M., Vezina, C., Flynn, G. C., Liu, Y. D., Rehder, D. S., Plant, M., Henkle, B., Li, Y., Deechongkit, S., Varnum, B., Wypych, J., Balland, A., and Bondarenko, P. V. (2008) Structural and functional characterization of disulfide isoforms of the human IgG2 subclass, *J. Biol. Chem.* . (published online).
14. Brady, L. J., Valliere-Douglass, J. F., Martinez, T., and Balland, A. (2008) Molecular mass analysis of antibodies by online SEC-MS. *J. ASMS 19*, 502–509.
15. Banfield, M. J., King, D. J., Mountain, A., and Brady, R. L. (1997) V_L:V_H domain rotations in engineered antibodies: crystal structures of the Fab fragments from two murine anti-tumor antibodies and their engineered human constructs. *Proteins 29*, 161–171.
16. Saphire, E. O., Parren, P. W. H. I., Pantophlet, R., Zwick, M. B., Morris, G. M., Rudd, P. M., Dwek, R. A., Stanfield, R. L., Burton, D. R., and Wilson, I. A. (2001) Crystal structure of a neutralizing human IgG against HIV-1: a template for vaccine design. *Science 293*, 1155–1159.
17. Guo, A., Han, M., Martinez, T., Ketchem, R., Jochheim, C., Novick, S., and Balland, A. (2008) Electrophoretic evidence for the presence of structural isoforms specific for the IgG2 isotype, *Electrophoresis* (in press).
18. Jefferis, R. (2005) Glycosylation of recombinant antibody therapeutics. *Biotechnol. Prog. 21*, 11–16.
19. Bures, E. J., Hui, J. O., Chow, D. T., Katta, V., Rohde, M. F., Zeni, L., Rosenfeld, R. D., Stark, K. L., and Haniu, M. (1998) Determination of disulfide structure in Agouti-related protein (AGRP) by stepwise reduction and alkylation. *Biochemistry 37*, 12172–12177.
20. Gray, W. R. (1993) Disulfide structures of highly bridged peptides: a new strategy for analysis. *Protein Sci. 2*, 1732–1748.
21. Roux, K. H., Strelets, L., and Michaelsen, T. E. (1997) Flexibility of IgG subclasses. *J. Immunol. 159*, 3372–3382.
22. Marchalonis, J. J., Schluter, S. F., Bernstein, R. M., Shen, S., and Edmunson, A. B. (1998) Phylogenetic emergence and molecular evolution of the immunoglobulin family. *Adv. Immunol. 70*, 417–506.
23. Sandin, S., Ofwerstedt, L. G., Wikstrom, A. C., Wrange, O., and Skoglund, U. (2004) Structure and flexibility of individual Immunoglobulin G molecules in solution. *Structure 12*, 409–415.
24. Yoo, E. M., Wims, L. A., Chan, L. A., and Morrison, S. L. (2003) Human IgG2 can form covalent dimers. *J. Immunol. 170*, 3134–3138.
25. Jefferis, R., and Lund, J. (2002) Interaction sites on human IgG-Fc for FcγR: current models. *Immunol. Lett. 82*, 57–65.
26. Chappel, M. S., Insenman, D. E., Everett, M., Xu, R., Dorrington, K. J., and Klein, M. H. (1991) Identification of the Fcγ receptor class I binding site in human IgG through the use of recombinant IgG1/IgG2 hybrid and point-mutated antibodies. *Proc. Natl. Acad. Sci. U.S.A. 88*, 9036–9040.
27. Sensel, M. G., Kane, L. M., and Morrison, S. L. (1997) Amino acid differences in the N-terminus of C_H2 influence the relative abilities of IgG2 and IgG3 to activate complement. *Mol. Immunol. 34*, 1019–1029.
28. Armour, K. L., van de Winkel, J. G. J., Williamson, L. M., and Clark, M. R. (2003) Differential binding to human FcγRIIa and FcγRIIb by human IgG wild type and mutant antibodies. *Mol. Immunol. 40*, 585–593.
29. Woof, J. M., and Burton, D. R. (2004) Human antibody-Fc receptor interactions illuminated by crystal structures. *Nat. Rev. Immunol. 4*, 1–11.

BI800576C